

Constraints on fast radio burst population from the first CHIME/FRB catalog with the Hierarchical Bayesian Inference

HUAN ZHOU,¹ ZHENGXIANG LI,^{2,3} AND ZONG-HONG ZHU^{1,2}

¹*Department of Astronomy, School of Physics and Technology, Wuhan University, Wuhan 430072, China*

²*Department of Astronomy, School of Physics and Astronomy, Beijing Normal University, Beijing 100875, China*

³*Institute for Frontiers in Astronomy and Astrophysics, Beijing Normal University, Beijing 102206, China*

ABSTRACT

Fast Radio Bursts (FRBs) have emerged as one of the most dynamic areas of research in astronomy and cosmology. Despite increasing number of FRBs have been reported, the exact origin of FRBs remains elusive. Investigating the intrinsic redshift distributions of FRBs could provide valuable insights into their possible origins and enhance the power of FRBs as a cosmological probe. In this paper, we propose a hierarchical Bayesian inference approach combining with several viable models to investigate the redshift distribution of the CHIME/FRB catalog 1. By utilizing this method, we aim to uncover the underlying patterns and characteristics of the FRB population, i.e. intrinsic redshift distribution of FRB. Taking uncertainties within the observational data and selection effects into consideration, we obtained that the redshift distribution of FRBs is significantly delayed with respect to that of the star formation history.

Keywords: Fast radio bursts, History of star formation.

1. INTRODUCTION

Fast Radio Bursts (FRBs) are bright radio transients with durations being a few milliseconds. Since first FRB (FRB 20010724) was discovered in 2007 (Lorimer et al. 2007), hundreds of FRBs have been detected by various radio telescopes, such as the Australian Square Kilometer Array Pathfinder (ASKAP), the Canadian Hydrogen Intensity Mapping Experiment (CHIME), the Five-hundred-meter Aperture Spherical radio telescope (FAST), and Deep Synoptic Array-110 (DSA-110), etc. While their radiation mechanism and progenitors remains unknown, several theories suggest they could be linked to exotic astrophysical phenomena such as magnetars, black holes or neutron star mergers (Petroff et al. 2019; Cordes & Chatterjee 2019; Zhang 2020; Xiao et al. 2021). However, several distinctive and valuable observational properties of FRBs, such as their short durations, cosmological origins, and high all-sky event rate, have been identified as potential probes for cosmology

and astrophysics (Gao et al. 2014; Wei et al. 2015; Muñoz et al. 2016; Li et al. 2018, 2020; Liao et al. 2020; Zhou et al. 2022).

The FRB population, i.e. the energy and the redshift distribution, has been extensively studied in many literatures (Zhang & Wang 2019; Pleunis et al. 2021; Zhang et al. 2021; James et al. 2022a,b; Qiang et al. 2022; Zhang & Zhang 2022; Shin et al. 2023; Zhang et al. 2023; Chen et al. 2024; Lin & Zou 2024a; Lin et al. 2024b; Gupta et al. 2025). Based on assumptions for dispersion measures (DMs) from host galaxies and the Milky Way halo, it was found that, independent of the redshift distribution, the intrinsic energy distribution of FRBs may follow a power law distribution with a high-energy exponential cutoff (Luo et al. 2020; Lu et al. 2020). However, due to different predictions of progenitor theories, the redshift distribution is not as clear as the energy distribution. For instance, a delayed FRB redshift distribution compared to the star formation history (SFH) was obtained from the FRB data detected by the Parkes and ASKAP (Zhang et al. 2021). Meanwhile, several independent studies also rule out the hypothesis that FRBs trace the SFH with the CHIME/FRB catalog 1, but the exact FRB population remains uncon-

zxli918@bnu.edu.cn

zhuzh@whu.edu.cn

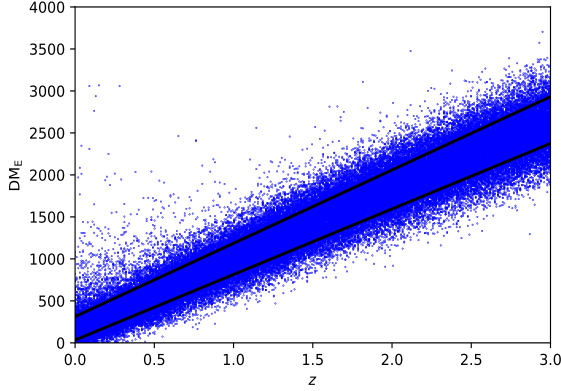


Figure 1. The blue scatter represents the $DM_E - z$ relation. The upper and lower black lines represent $\sigma_+(z)$ and $\sigma_-(z)$ in 1σ confidence region, respectively.

strained (Zhang & Wang 2019; Qiang et al. 2022; Zhang & Zhang 2022; Chen et al. 2024; Lin & Zou 2024a; Lin et al. 2024b; Gupta et al. 2025). Above all, the intrinsic redshift distribution of FRBs remains a topic of extensive debate.

In this paper, compared with the Kolmogorov-Smirnov (KS) test method (Qiang et al. 2022; Zhang & Zhang 2022) and Bayesian method with the cumulative distribution function (Lin & Zou 2024a; Lin et al. 2024b), we propose the hierarchical Bayesian inference (HBI) method to investigate the characteristics of the FRB population on the basis of the well-measured FRB catalog 1 reported by CHIME (Amiri et al. 2021). This paper is organized as follows: In Section 2, we introduce the FRB observations and the hierarchical Bayesian inference used to derive constraints on the population hyperparameters of FRB. In Section 3, we apply this approach to the selected FRB data and present the corresponding results. Finally, Section 4 presents conclusions and discussions. Throughout this paper, we use the concordance Λ CDM cosmology with the best-fitting parameters from the latest *Planck* cosmic microwave background (CMB) observations (Aghanim et al. 2020).

2. METHODOLOGY

2.1. Fast Radio Burst Population Models

The redshift distribution of Fast Radio Bursts (FRBs) can be inferred using the dispersion measure (DM) as a proxy. DM is the integral of the free electron number density along the line of sight, and it can be directly obtained from the dynamical spectra of the burst. The distance and redshift of a detected FRB can be approximately estimated from its observed DM, which is proportional to the number density of free electron along the line of sight and is usually decomposed into the fol-

lowing three ingredients (Deng & Zhang 2014; Macquart et al. 2020),

$$DM_{\text{obs}} = DM_{\text{MW}} + DM_{\text{IGM}} + \frac{DM_{\text{host}}}{1+z}. \quad (1)$$

DM_{MW} is the contribution from the Milky Way as

$$DM_{\text{MW}} = DM_{\text{MW,ISM}} + DM_{\text{MW,halo}}, \quad (2)$$

where $DM_{\text{MW,ISM}}$ interstellar medium, which can be estimated using the Milky Way electron density models, such as the NE2001 model (Cordes & Lazio 2002) and YMW16 model ¹ (Yao et al. 2017). Previous studies suggested that sources with low DM imply small contributions, $\sim 25 \text{ pc cm}^{-3}$, from the halos of M81 and the Milky Way (Bhardwaj et al. 2021; Cordes et al. 2022). Therefore, $DM_{\text{MW,halo}}$ is approximately estimated to be 25 pc cm^{-3} in this paper. DM_{IGM} represents DM contribution from intergalactic medium (IGM). In the standard Λ CDM model the average value of the DM_{IGM} can be calculated as (Deng & Zhang 2014)

$$\langle DM_{\text{IGM}}(z) \rangle = \frac{3H_0\Omega_b f_{\text{IGM}} f_e}{8\pi m_p} \times \int_0^z \frac{1+z}{\sqrt{\Omega_m(1+z)^3 + \Omega_\Lambda}} dz, \quad (3)$$

where H_0 is the Hubble constant, Ω_m is the present-day matter density, m_p is the proton mass, $f_{\text{IGM}} = 0.84$ is the baryon mass fraction in IGM, and $f_e = 7/8$ is the electron fraction. Following previous works (Qiang & Wei 2020), we consider the σ_{IGM} was given by a simple power-law function as

$$\sigma_{\text{IGM}} \approx 173.8z^{0.4} \text{ pc cm}^{-3}. \quad (4)$$

In addition, DM_{host} represents the contribution from host galaxy, and it is usually modeled as a log-normal distribution (Macquart et al. 2020)

$$p(DM_{\text{host}}|\mu_h, \sigma_h) = \frac{1}{\sqrt{2\pi DM_{\text{host}} \sigma_h}} \times \exp \left[-\frac{(\ln(DM_{\text{host}}) - \mu_h)^2}{2\sigma_h^2} \right] \quad (5)$$

where the parameters μ_h and σ_h are the mean and standard deviation of $\ln(DM_{\text{host}})$, and Tang et al. (2023) has given the well constrains (μ_h, σ_h) from 17 well-localized FRBs (Tang et al. 2023). Thus, subtracting the known DM_{MW} from DM_{obs} in Equation (1), it is convenient

¹ We have tested the influence of these two models on our results and found that the impact is negligible. Therefore, our following analysis are based on the NE2001 model.

to introduce the extragalactic DM_E of an FRB as the observed quantity

$$\text{DM}_E \equiv \text{DM}_{\text{IGM}} + \frac{\text{DM}_{\text{host}}}{1+z}. \quad (6)$$

As shown in Figure 1, the blue scatter represents the $\text{DM}_E - z$ relation which is inferred from the contributions of DM_{IGM} and DM_{host} with their uncertainties. In addition, $\sigma_+(z)$ (the upper black line in Figure 1) and $\sigma_-(z)$ (the lower black line in Figure 1) represent the best polynomial fit of the boundary of 1σ confidence region for the $\text{DM}_E - z$ relation, respectively.

The observed FRB redshift rate distribution is from the intrinsic event rate density of FRB $dN/(dtdV) \equiv \mathcal{R}(z|\Phi)$, the most well-motivated model is the SFH model. Based on the gamma-ray burst population does not track SFH and the enhanced evolution in the GRB rate can be parameterized as $\mathcal{R}(z) \propto \varepsilon(z)\text{SFH}(z)$ (Kistler et al. 2008; Yuksel et al. 2008), we adopt three kinds of best-fit SFH-related models discussed in previous studies (Qiang et al. 2022; Lin & Zou 2024a).

• **1. Two-segment (TSE) model:**

$$\mathcal{R}(z|\gamma_1, \gamma_2, z_t) = R_{\text{TSE},0} \times \frac{(1+z)^{\gamma_1}}{1 + ((1+z)/(1+z_t))^{\gamma_1+\gamma_2}} \text{SFH}(z), \quad (7)$$

where $R_{\text{TSE},0}$ is the local event rate in $\text{Gpc}^{-3}\text{yr}^{-1}$, and $\text{SFH}(z)$ is the empirical SFH model (Madau & Fragos 2017) as

$$\text{SFH}(z) = \frac{(1+z)^{2.6}}{1 + ((1+z)/3.2)^{6.2}}, \quad (8)$$

which is expected to behave like $(1+z)^{2.6}$ and $(1+z)^{-3.6}$ at low and high redshifts respectively.

• **2. Power law with an exponential cutoff (CPL) model:**

$$\mathcal{R}(z|\gamma, z_c) = R_{\text{CPL},0} \times \frac{(1+z)^\gamma \exp(-z/z_c)}{(1+z)^\gamma} \text{SFH}(z), \quad (9)$$

which is expected to behave like $(1+z)^{2.6+\gamma}$ and exponential cutoff at low and high redshifts respectively.

• **3. Non-SFH-based two-segment redshift distribution (TSRD) model:**

$$\mathcal{R}(z|\lambda, \kappa, z_p) = R_{\text{TSRD},0} \times \frac{(1+z)^\lambda}{1 + ((1+z)/(1+z_p))^{\lambda+\kappa}}, \quad (10)$$

if z_p is much larger than 0 and $\lambda + \kappa$ is positive, this model is expected to behave like $(1+z)^\lambda$ and $(1+z)^{-\kappa}$ at low and high redshifts respectively.

Therefore, the population hyperparameters of three models Φ are

$$\Phi = [\gamma_1, \gamma_2, z_t, \gamma, z_c, \lambda, \kappa, z_p]. \quad (11)$$

Consistent with previous works, we set similar prior distributions for all the hyperparameters Φ as shown in Table 1.

Model	Hyperparameter Φ	Prior
TSE	γ_1	$\mathcal{U}[-10, 10]$
	γ_2	$\mathcal{U}[-10, 10]$
	z_t	$\mathcal{U}[0, 10]$
CPL	γ	$\mathcal{U}[-10, 10]$
	z_c	$\mathcal{U}[0, 10]$
TSRD	λ	$\mathcal{U}[-10, 10]$
	κ	$\mathcal{U}[-10, 10]$
	z_p	$\mathcal{U}[0, 10]$

Table 1. Population hyperparameters $\Phi = [\gamma_1, \gamma_2, z_t, \gamma, z_c, \lambda, \kappa, z_p]$ and their prior distributions used in the HBI.

2.2. Hierarchical Bayesian Inference

For population hyperparameters of FRB Φ , and N_{obs} detections of FRB events $d = [d_1, \dots, d_{N_{\text{obs}}}]$ ², the likelihood follows a Poisson distribution without considering measurement uncertainty and selection effect is

$$p(d|\Phi) \propto N(\Phi)^{N_{\text{obs}}} e^{-N(\Phi)}. \quad (12)$$

However, with measurement uncertainty and selection effect taken into account, the likelihood for N_{obs} FRB observations can be characterized by the inhomogeneous Poisson process as (Mandel et al. 2019; Abbott et al. 2023; Mastroianni et al. 2024)

$$p(d|\Phi) \propto N(\Phi)^{N_{\text{obs}}} e^{-N(\Phi)\xi(\Phi)} \times \prod_i^{N_{\text{obs}}} \int dz L(d_i|z) p_{\text{pop}}(z|\Phi), \quad (13)$$

² In later analysis, d_i represents the DM for single observed non-repeating FRB event in CHIME catalog 1.

where $L(d_i|z)$ is the likelihood of one FRB. We assume the likelihood $L(d_i|z)$ for data follows the Gaussian distribution with the error coming from DM_{IGM} and DM_{host} as

$$L(d_i|z) = \frac{1}{\sqrt{2\pi}\sigma_{z,i}} \exp\left[-\frac{(z - \bar{z}_i)^2}{2\sigma_{z,i}^2}\right], \quad (14)$$

where \bar{z}_i and $\sigma_{z,i}$ come from the $\text{DM}_{\text{E}} - z$ relation of each FRB as

$$\begin{aligned} \bar{z} &= \frac{\sigma_+^{-1}(\text{DM}_{\text{E}}) + \sigma_-^{-1}(\text{DM}_{\text{E}})}{2} \\ \sigma_z &= \frac{\sigma_+^{-1}(\text{DM}_{\text{E}}) - \sigma_-^{-1}(\text{DM}_{\text{E}})}{2}, \end{aligned} \quad (15)$$

where $\sigma_+^{-1}(\text{DM}_{\text{E}})$ and $\sigma_-^{-1}(\text{DM}_{\text{E}})$ represent the inverse function of the best polynomial fit for $\sigma_+(z)$ and $\sigma_-(z)$ shown in Figure 1, respectively. In Equation (13), $N(\Phi)$ is the total number of FRBs in the model characterized by the set of population parameters Φ as

$$N(\Phi) = \int dz T_{\text{obs}} \mathcal{R}(\lambda|\Phi) \frac{1}{1+z} \frac{dV_c}{dz}, \quad (16)$$

where dV_c/dz is the differential comoving volume, the factor $1/(1+z)$ accounts for the cosmological time dilation from the source frame to the detector frame, and we define T_{obs} as the effective observing time which is 100% operational time of CHIME³. In addition, $p_{\text{pop}}(z|\Phi)$ is the normalized distribution of redshifts in FRBs as

$$p_{\text{pop}}(z|\Phi) = \frac{1}{N(\Phi)} \left[T_{\text{obs}} \mathcal{R}(z|\Phi) \frac{1}{1+z} \frac{dV_c}{dz} \right]. \quad (17)$$

Meanwhile, the detected fraction $\xi(\Phi)$ of FRBs observed by the CHIME telescope can be defined as

$$\xi(\Phi) \equiv \int dz P_{\text{det}}(z) p_{\text{pop}}(z|\Phi), \quad (18)$$

where $P_{\text{det}}(z)$ is the detection probability that depends on the source and instrument. The selection effect of the CHIME telescope is determined by detection efficiency as a function η_{det} of the specific fluence (Zhang & Zhang 2022; Qiang et al. 2022; Lin & Zou 2024a; Lin et al. 2024b)

$$\eta_{\text{det}}(F_\nu) = \left(\frac{\log(F_\nu) - \log(F_{\nu,\min})}{\log(F_{\nu,\max}) - \log(F_{\nu,\min})} \right)^n. \quad (19)$$

This model assumes a ‘grey zone’ between the minimum specific threshold fluence $F_{\nu,\min}$, and the maximum specific threshold fluence $F_{\nu,\max}$. FRBs with $F_\nu < F_{\nu,\min}$,

are undetectable hence $\eta_{\text{det}} = 0$, while above $F_{\nu,\max}$ all FRBs are detectable hence $\eta_{\text{det}} = 1$. Assuming a flat radio spectrum, the observed specific fluence F_ν for a mock FRB with redshift z and isotropic energy E is (Zhang 2018; James et al. 2022a; Zhang et al. 2021)

$$F_\nu = \frac{(1+z)^{2+\beta}}{4\pi d_L^2 \Delta\nu} E, \quad (20)$$

where β is the spectrum index $F_\nu \propto \nu^\beta$, d_L is the luminosity distance, and $\Delta\nu$ is the bandwidth in which the FRB is detected. Macquart et al. (2019) have fitted β with 23 FRBs detected by ASKAP in Fly’s Eye mode, finding best-fit value $\beta = -1.5$. Like Luo et al. (2020); Lu et al. (2020), we assume the model of energy function $p(E)$ as power-law with high-energy exponential cutoff

$$p(E) = \Phi_0 \left(\frac{E}{E_c} \right)^{-\alpha} \exp\left(-\frac{E}{E_c}\right), \quad (21)$$

where α is the **power-law index**, E_c is the break energy, and Φ_0 is a normalization constant. Previous works showed that $\alpha \sim 1.8$ is consistent with observations (Luo et al. 2020; Lu et al. 2020), and Luo et al. (2020) suggested an energy cut-off at $E_c \sim 3 \times 10^{41} \text{erg}$. By marginalizing the local event rate ($R_{\text{TSE},0}$, $R_{\text{CPL},0}$, $R_{\text{TRSD},0}$) with a log-uniform prior for it, the posterior distribution $p(\Phi|d)$ could be obtained

$$\begin{aligned} p(\Phi|d) &= \frac{p(d|\Phi)p(\Phi)}{Z_{\mathcal{M}}} \\ &\propto \frac{p(\Phi)}{Z_{\mathcal{M}}} \xi(\Phi)^{-N_{\text{obs}}} \prod_i^{N_{\text{obs}}} \int dz L(d_i|z) p_{\text{pop}}(z|\Phi), \end{aligned} \quad (22)$$

where $Z_{\mathcal{M}}$ is the Bayesian evidence for the population model \mathcal{M} , $p(\Phi)$ is prior distribution for the hyperparameters Φ .

3. RESULTS

In this section, we use the first CHIME/FRB catalog with well measured DM_{obs} to constrain FRB population hyperparameters, which are detected from 2018 July 25 to 2019 July 1⁴ (Amiri et al. 2021). The first CHIME/FRB catalog contains 536 bursts in total, i.e. 474 non-repeating bursts and 62 repeating bursts corresponding to 18 different FRB sources. Similar to previous works (Zhang & Zhang 2022; Qiang et al. 2022; Lin & Zou 2024a; Lin et al. 2024b), here we only select the FRBs with $\text{DM}_{\text{E}} \geq 200 \text{ pc cm}^{-3}$ (in total 415 FRBs).

Then we incorporate the above-mentioned FRBs sample into the **EMCEE** (Foreman-Mackey et al. 2013)

³ CHIME operates nominally 24 hr per day during 25 July 2018 and 1 July 2019, but CHIME was not fully operational 100% of the time as some reasons shown in Section 2.2 (Amiri et al. 2021)

⁴ <https://www.chime-frb.ca/catalog>

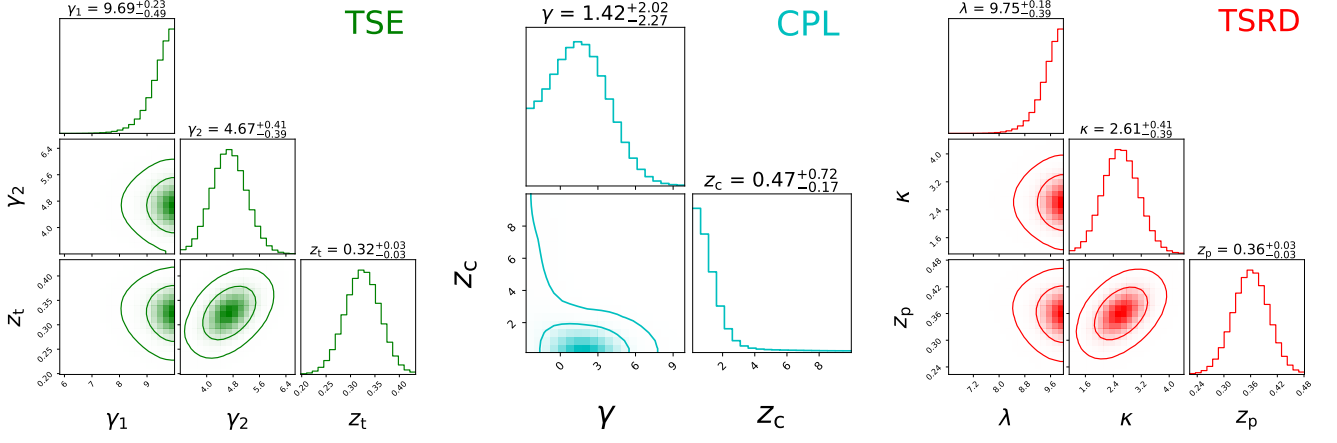


Figure 2. The contour plot with 2σ uncertainty for the TSE model (left), CPL model (middle) and TSRD model (right).

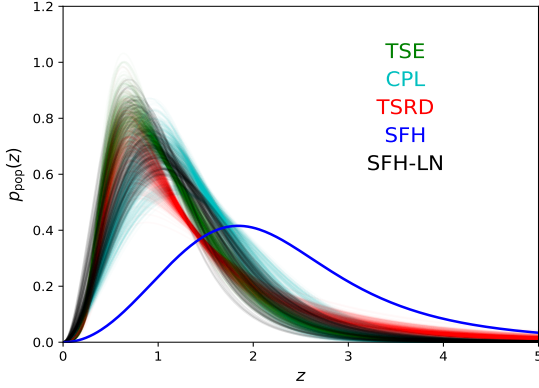


Figure 3. The redshift distribution of FRBs derived from the reconstruction procedure with the posterior distributions for TSE, CPL and TSRD models respectively. For comparison, we also give the redshift distribution from SFH model.

with the posterior Equation (22) to estimate population hyperparameters ($\Phi = [\gamma_1, \gamma_2, z_t, \gamma, z_c, \lambda, \kappa, z_p]$) from three models. Our results are summarized in Figure 2 and Table 2. We find that the inferred FRB redshift distribution is tilted lower away from the predicted SFH peak, which is consistent with Lin & Zou (2024a); Lin et al. (2024b) works. To quantify the goodness of three models, we perform model comparison statistics by using the Bayesian Information Criterion (BIC) (Schwarz 1978), which is expressed as

$$\text{BIC}_{\mathcal{M}} = -2 \ln(\mathcal{L}_{\max, \mathcal{M}}) + k_{\mathcal{M}} \ln(N_{\text{obs}}), \quad (23)$$

where $k_{\mathcal{M}}$ represent the total number of population hyperparameters, and $\mathcal{L}_{\max, \mathcal{M}}$ is the maximum likelihood $p(d|\Phi)$ value for the N_{obs} FRB events in the framework of \mathcal{M} model. $\Delta\text{BIC} \geq 5$ or ≥ 10 indicates that there is “strong” or “decisive” evidence against the considered model with respect to the fiducial model. With the results listed in Table 2, we have the rank of fits as

$\text{TSRD} \gtrsim \text{TSE} \gg \text{CPL}$. However, we find that the constraints of some hyperparameters in the three models, i.e. γ_1 , γ , and λ , tend to be larger in range, which indicates that the redshift distribution of FRBs is steeper in the low redshift interval.

In order to compare the SFH model and its time delay model, the redshift distributions of FRBs derived from the reconstruction with the posterior distributions for three kind of models have shown in Figure 3. In Figure 3, SFH-LN represents the redshift distribution corresponding to the SFH model with the log-normal time delay distribution $f(t|\tau_0, \sigma_0)$ as

$$\mathcal{R}(z) \propto \int_0^{t_{\max}} \text{SFH}(t(z) - t_d) f(t_d|\tau_0, \sigma_0) dt_d. \quad (24)$$

For the sake of comparison, we also take the parameters τ_0 and σ_0 as uniform distributions $\mathcal{U}[5, 10]$ Gyr and $\mathcal{U}[0.8, 1.5]$, respectively. We find that the distributions of FRBs from our results do not trace the history of star formation, and there is the tendency for the redshift distribution of FRBs to favor SFH model with a time delay. Moreover, this is consistent with conclusions from Zhang & Zhang (2022); Chen et al. (2024); Lin et al. (2024b); Gupta et al. (2025) works.

4. CONCLUSIONS AND DISCUSSION

Nowadays, FRBs have become one of the most significant probes for astrophysical and cosmological purposes. However, the origin of FRBs remains unknown. Studies of the intrinsic FRB distributions may provide insights into their possible origins. In this paper, based on FRB data from the first CHIME/FRB catalog, we propose the HBI method to constrain the FRB population information, i.e. intrinsic redshift distribution of FRB. We find the current FRB sample does not trace the history of star formation. This conclusion is consistent with the findings of many previous studies (Zhang & Wang 2019;

Model	Hyperparameter Φ	ΔBIC
TSE	$\gamma_1 = 9.69^{+0.23}_{-0.49}$	0
	$\gamma_2 = 4.67^{+0.41}_{-0.39}$	
	$z_t = 0.32^{+0.03}_{-0.03}$	
CPL	$\gamma = 1.42^{+2.02}_{-2.27}$	98.87
	$z_c = 0.47^{+0.72}_{-0.17}$	
TSRD	$\lambda = 9.75^{+0.18}_{-0.39}$	-2.10
	$\kappa = 2.61^{+0.41}_{-0.39}$	
	$z_p = 0.36^{+0.03}_{-0.03}$	

Table 2. The optimal Population hyperparameters $\Phi = [\gamma_1, \gamma_2, z_t, \gamma, z_c, \lambda, \kappa, z_p]$ and their 1σ uncertainties. For comparing the TSE population model with other models, we also list ΔBIC .

Zhang et al. 2021; Qiang et al. 2022; Zhang & Zhang 2022; Zhang et al. 2023; Chen et al. 2024; Lin & Zou 2024a; Lin et al. 2024b; Gupta et al. 2025), which is also understandable, because the current inferred redshift distribution of is mostly concentrated below 2.

With the rapid increase of the number of FRBs detected by powerful wide-field surveys (like CHIME, SKA,

and DSA-110) and more stringent restrictions on the FRB host environment in the future, the population characteristics of FRBs will be increasingly restricted, which will help us to study their origins. In addition, similar to using compact object populations and gravitational wave events in GWTC-3 to limit cosmological models (Abbott et al. 2023; Mastrogiiovanni et al. 2024), since DM_E of FRB contains cosmological information, it is foreseen that FRB can also be take as a “dark siren” for constraining cosmology.

5. ACKNOWLEDGEMENTS

We are grateful to Dachun Qiang for helpful discussion. This work is supported by the China National Postdoctoral Program for Innovative Talents under Grant No.BX20230271; National Key Research and Development Program under Grant No.2024YFC2207400; National Key Research and Development Program of China Grant No. 2021YFC2203001; National Natural Science Foundation of China under Grants Nos.11920101003, 12021003, 11633001, 12322301, and 12275021; the Strategic Priority Research Program of the Chinese Academy of Sciences, Grant Nos. XDB2300000 and the Interdiscipline Research Funds of Beijing Normal University.

REFERENCES

- Abbott, R., et al. 2023, Phys. Rev. X, 13, 011048, doi: [10.1103/PhysRevX.13.011048](https://doi.org/10.1103/PhysRevX.13.011048)
- Aghanim, N., et al. 2020, Astron. Astrophys., 641, A6, doi: [10.1051/0004-6361/201833910](https://doi.org/10.1051/0004-6361/201833910)
- Amiri, M., et al. 2021, Astrophys. J. Supp., 257, 59, doi: [10.3847/1538-4365/ac33ab](https://doi.org/10.3847/1538-4365/ac33ab)
- Bhardwaj, M., Gaensler, B. M., Kaspi, V. M., et al. 2021, ApJL, 910, L18, doi: [10.3847/2041-8213/abeaa6](https://doi.org/10.3847/2041-8213/abeaa6)
- Chen, J. H., Jia, X. D., Dong, X. F., & Wang, F. Y. 2024, Astrophys. J. Lett., 973, L54, doi: [10.3847/2041-8213/ad7b39](https://doi.org/10.3847/2041-8213/ad7b39)
- Cordes, J. M., & Chatterjee, S. 2019, Ann. Rev. Astron. Astrophys., 57, 417, doi: [10.1146/annurev-astro-091918-104501](https://doi.org/10.1146/annurev-astro-091918-104501)
- Cordes, J. M., & Lazio, T. J. W. 2002, <https://arxiv.org/abs/astro-ph/0207156>
- Cordes, J. M., Ocker, S. K., & Chatterjee, S. 2022, Astrophys. J., 931, 88, doi: [10.3847/1538-4357/ac6873](https://doi.org/10.3847/1538-4357/ac6873)
- Deng, W., & Zhang, B. 2014, Astrophys. J. Lett., 783, L35, doi: [10.1088/2041-8205/783/2/L35](https://doi.org/10.1088/2041-8205/783/2/L35)
- Foreman-Mackey, D., Hogg, D. W., Lang, D., & Goodman, J. 2013, Publ. Astron. Soc. Pac., 125, 306, doi: [10.1086/670067](https://doi.org/10.1086/670067)
- Gao, H., Li, Z., & Zhang, B. 2014, Astrophys. J., 788, 189, doi: [10.1088/0004-637X/788/2/189](https://doi.org/10.1088/0004-637X/788/2/189)
- Gupta, O., Beniamini, P., Kumar, P., & Finkelstein, S. L. 2025, <https://arxiv.org/abs/2501.09810>
- James, C. W., Prochaska, J. X., Macquart, J. P., et al. 2022a, Mon. Not. Roy. Astron. Soc., 509, 4775, doi: [10.1093/mnras/stab3051](https://doi.org/10.1093/mnras/stab3051)
- . 2022b, Mon. Not. Roy. Astron. Soc., 510, L18, doi: [10.1093/mnrasl/slab117](https://doi.org/10.1093/mnrasl/slab117)
- Kistler, M. D., Yuksel, H., Beacom, J. F., & Stanek, K. Z. 2008, Astrophys. J. Lett., 673, L119, doi: [10.1086/527671](https://doi.org/10.1086/527671)
- Li, Z., Gao, H., Wei, J.-J., et al. 2020, Mon. Not. Roy. Astron. Soc., 496, L28, doi: [10.1093/mnrasl/slaa070](https://doi.org/10.1093/mnrasl/slaa070)
- Li, Z.-X., Gao, H., Ding, X.-H., Wang, G.-J., & Zhang, B. 2018, Nature Commun., 9, 3833, doi: [10.1038/s41467-018-06303-0](https://doi.org/10.1038/s41467-018-06303-0)
- Liao, K., Zhang, S. B., Li, Z., & Gao, H. 2020, Astrophys. J., 896, L11, doi: [10.3847/2041-8213/ab963e](https://doi.org/10.3847/2041-8213/ab963e)

- Lin, H.-N., Li, X.-Y., & Zou, R. 2024b, *Astrophys. J.*, 969, 123, doi: [10.3847/1538-4357/ad5310](https://doi.org/10.3847/1538-4357/ad5310)
- Lin, H.-N., & Zou, R. 2024a, *Astrophys. J.*, 962, 73, doi: [10.3847/1538-4357/ad1b4f](https://doi.org/10.3847/1538-4357/ad1b4f)
- Lorimer, D. R., Bailes, M., McLaughlin, M. A., Narkevic, D. J., & Crawford, F. 2007, *Science*, 318, 777, doi: [10.1126/science.1147532](https://doi.org/10.1126/science.1147532)
- Lu, W., Piro, A. L., & Waxman, E. 2020, *Mon. Not. Roy. Astron. Soc.*, 498, 1973, doi: [10.1093/mnras/staa2397](https://doi.org/10.1093/mnras/staa2397)
- Luo, R., Men, Y., Lee, K., et al. 2020, *Mon. Not. Roy. Astron. Soc.*, 494, 665, doi: [10.1093/mnras/staa704](https://doi.org/10.1093/mnras/staa704)
- Macquart, J. P., Shannon, R. M., Bannister, K. W., et al. 2019, *Astrophys. J. Lett.*, 872, L19, doi: [10.3847/2041-8213/ab03d6](https://doi.org/10.3847/2041-8213/ab03d6)
- Macquart, J. P., et al. 2020, *Nature*, 581, 391, doi: [10.1038/s41586-020-2300-2](https://doi.org/10.1038/s41586-020-2300-2)
- Madau, P., & Fragos, T. 2017, *Astrophys. J.*, 840, 39, doi: [10.3847/1538-4357/aa6af9](https://doi.org/10.3847/1538-4357/aa6af9)
- Mandel, I., Farr, W. M., & Gair, J. R. 2019, *Mon. Not. Roy. Astron. Soc.*, 486, 1086, doi: [10.1093/mnras/stz896](https://doi.org/10.1093/mnras/stz896)
- Mastrogiovanni, S., Pierra, G., Perriès, S., et al. 2024, *Astron. Astrophys.*, 682, A167, doi: [10.1051/0004-6361/202347007](https://doi.org/10.1051/0004-6361/202347007)
- Muñoz, J. B., Kovetz, E. D., Dai, L., & Kamionkowski, M. 2016, *Phys. Rev. Lett.*, 117, 091301, doi: [10.1103/PhysRevLett.117.091301](https://doi.org/10.1103/PhysRevLett.117.091301)
- Petroff, E., Hessels, J. W. T., & Lorimer, D. R. 2019, *Astron. Astrophys. Rev.*, 27, 4, doi: [10.1007/s00159-019-0116-6](https://doi.org/10.1007/s00159-019-0116-6)
- Pleunis, Z., et al. 2021, *Astrophys. J.*, 923, 1, doi: [10.3847/1538-4357/ac33ac](https://doi.org/10.3847/1538-4357/ac33ac)
- Qiang, D.-C., Li, S.-L., & Wei, H. 2022, *JCAP*, 01, 040, doi: [10.1088/1475-7516/2022/01/040](https://doi.org/10.1088/1475-7516/2022/01/040)
- Qiang, D.-C., & Wei, H. 2020, *JCAP*, 04, 023, doi: [10.1088/1475-7516/2020/04/023](https://doi.org/10.1088/1475-7516/2020/04/023)
- Schwarz, G. 1978, *Annals Statist.*, 6, 461
- Shin, K., et al. 2023, *Astrophys. J.*, 944, 105, doi: [10.3847/1538-4357/acaf06](https://doi.org/10.3847/1538-4357/acaf06)
- Tang, L., Lin, H.-N., & Li, X. 2023, *Chin. Phys. C*, 47, 085105, doi: [10.1088/1674-1137/acda1c](https://doi.org/10.1088/1674-1137/acda1c)
- Wei, J.-J., Gao, H., Wu, X.-F., & Mészáros, P. 2015, *Phys. Rev. Lett.*, 115, 261101, doi: [10.1103/PhysRevLett.115.261101](https://doi.org/10.1103/PhysRevLett.115.261101)
- Xiao, D., Wang, F., & Dai, Z. 2021, *Sci. China Phys. Mech. Astron.*, 64, 249501, doi: [10.1007/s11433-020-1661-7](https://doi.org/10.1007/s11433-020-1661-7)
- Yao, J. M., Manchester, R. N., & Wang, N. 2017, *Astrophys. J.*, 835, 29, doi: [10.3847/1538-4357/835/1/29](https://doi.org/10.3847/1538-4357/835/1/29)
- Yuksel, H., Kistler, M. D., Beacom, J. F., & Hopkins, A. M. 2008, *Astrophys. J. Lett.*, 683, L5, doi: [10.1086/591449](https://doi.org/10.1086/591449)
- Zhang, B. 2018, *Astrophys. J. Lett.*, 867, L21, doi: [10.3847/2041-8213/aae8e3](https://doi.org/10.3847/2041-8213/aae8e3)
- . 2020, *Nature*, 587, 45, doi: [10.1038/s41586-020-2828-1](https://doi.org/10.1038/s41586-020-2828-1)
- Zhang, G. Q., & Wang, F. Y. 2019, *Mon. Not. Roy. Astron. Soc.*, 487, 3672, doi: [10.1093/mnras/stz1566](https://doi.org/10.1093/mnras/stz1566)
- Zhang, J., Zhang, C., Li, D., et al. 2023, *Astron. Rep.*, 67, 244, doi: [10.1134/S1063772923030083](https://doi.org/10.1134/S1063772923030083)
- Zhang, R. C., & Zhang, B. 2022, *Astrophys. J. Lett.*, 924, L14, doi: [10.3847/2041-8213/ac46ad](https://doi.org/10.3847/2041-8213/ac46ad)
- Zhang, R. C., Zhang, B., Li, Y., & Lorimer, D. R. 2021, *Mon. Not. Roy. Astron. Soc.*, 501, 157, doi: [10.1093/mnras/staa3537](https://doi.org/10.1093/mnras/staa3537)
- Zhou, H., Li, Z., Liao, K., et al. 2022, *Astrophys. J.*, 928, 124, doi: [10.3847/1538-4357/ac510d](https://doi.org/10.3847/1538-4357/ac510d)